Articles

Structural and Spectral Response of *Aequorea victoria* Green Fluorescent Proteins to Chromophore Fluorination†

Prajna P. Pal,‡ Jae Hyun Bae,§ M. Kamran Azim,|| Petra Hess,‡ Rainer Friedrich,‡ Robert Huber,‡ Luis Moroder,‡ and Nediljko Budisa*,‡

Max-Planck-Institut für Biochemie, Am Klopferspitz 18a, 82152 Martinsried, Germany, Department of Pharmacology, Yale University School of Medicine, New Haven, Connecticut 06520, and HEJ Research Institute of Chemistry, University of Karachi, Karachi 75270, Pakistan

Received July 16, 2004; Revised Manuscript Received November 26, 2004

ABSTRACT: Global replacements of tyrosine by 2- and 3-fluorotyrosine in "enhanced green" and "enhanced yellow" mutants of *Aequorea victoria* green fluorescent proteins (*av*GFPs) provided protein variants with novel biophysical properties. While crystallographic and modeled structures of these proteins are indistinguishable from those of their native counterparts (i.e., they are perfectly isomorphous), there are considerable differences in their spectroscopic properties. The fluorine being an integral part of the *av*GFP chromophore induces changes in the titration curves, variations in the intensity of the absorbance and fluorescence, and spectral shifts in the emission maxima. Furthermore, targeted fluorination in close proximity to the fluorinated chromophore yielded additional variants with considerably enhanced spectral changes. These unique spectral properties are intrinsic features of the fluorinated *av*GFPs, in the context of the rigid chromophore−microenvironment interactions. The availability of the isomorpohous crystal structures of fluorinated *av*GFPs allowed mapping of novel, unusual interaction distances created by the presence of fluorine atoms. In addition, fluorine atoms in the *ortho* position of the chromophore tyrosyl moiety exhibit a single conformation, while in the *meta* position two conformer states were observed in the crystalline state. Such global replacements in chromophores of *av*GFPs and similar proteins result in "atomic mutations" (i.e., H → F replacements) in the structures, offering unprecedented opportunities to understand and manipulate the relationships between protein structure and spectroscopic properties.

Naturally occurring halogen-containing amino acids such as iodinated tyrosines as precursors of thyroxine have been studied for decades in medicine (*1*). However, among thousands of halogenated substances present in nature, there are only a few organofluorine compounds that participate in the chemistry of living cells, despite fluorine being one of the most abundant elements in the earth's crust (*2*). Conversely, a wide variety of synthetic fluorinated compounds including fluorine-containing amino acids have been available for a long time. Synthetic fluoro derivatives of tyrosine (Tyr) were extensively used in protein ^{19}F NMR spectroscopy (*3*, *4*) and in biomedicine due to their capacity to act as antimetabolites (*5*).

Recently, biosynthetic incorporation of noncanonical amino acids in vitro has dramatically expanded the scope of protein structure/function studies (*6*). New developments in this field allow for in vivo generation of proteins with an expanded repertoire of amino acid residues since the cells are not always equipped to discriminate between canonical and noncanonical amino acids in protein biosynthesis. By exploiting this feature, Brooks and co-workers recently succeeded to incorporate 2-fluorotyrosine and 2,3-difluorotyrosine in plasmid-encoded ketosteroid isomerase using a Tyr-auxotrophic *Escherichia coli* strain (*7*). In the present study, (2-F)Tyr[1]- and (3-F)Tyr-containing green fluorescent proteins (GFPs) from jellyfish *Aequorea victoria* (*av*GFPs) were expressed by using the Tyr-auxotrophic *E. coli* host strain AT2471. Quantitative replacement of Tyr residues was

† This work was supported by SFB533 of the Ludwig-Maximilian University, Munich.

* To whom correspondence should be addressed. Phone: +49-89-8578-2661. Fax: +49-89-8578-3557. E-mail: budisa@biochem.mpg.de.

‡ Max-Planck-Institut für Biochemie.

§ Yale University School of Medicine.

|| University of Karachi.

[1] Abbreviations: *av*GFP, green fluorescent protein from *A. victoria*; EGFP, enhanced green fluorescent protein (Phe64Leu/Ser65Thr); EYFP, enhanced yellow fluorescent protein (Ser65Gly/Val68Leu/Ser72Ala/Thr203Tyr); ECFP, enhanced cyan fluorescent protein (Ser65Thr/Tyr66Trp/Phe64Leu/Asn146Ile/Met153Thr/Val163Ala); SPI, selective pressure incorporation method; NMM, new minimal medium; (2-F)-Tyr, 2-fluoro-L-tyrosine; (3-F)Tyr, 3-fluoro-L-tyrosine; IPTG, isopropyl thio-β-D-galactoside; ESI-MS, electrospray mass spectrometric analysis. *Mutant* denotes a protein in which the wild-type sequence is changed by site-directed mutagenesis (codon manipulation at the DNA level) in the frame of the standard amino acid repertoire (e.g., EGFP, EYFP, ECFP). *Variant* denotes a protein in which a single amino acid or multiple canonical amino acids from a wild-type or mutant sequence are replaced with noncanonical ones (expanded amino acid repertoire, codon reassignment at the protein translation level, e.g., (2-F)Tyr-EGFP, (3-F)Tyr-EGFP, etc.). In this work ECFP, ECFP, and EYFP are denoted as "parent" proteins when compared with variants derived from them.

10.1021/bi0484825 CCC: $30.25
Published on Web 02/11/2005

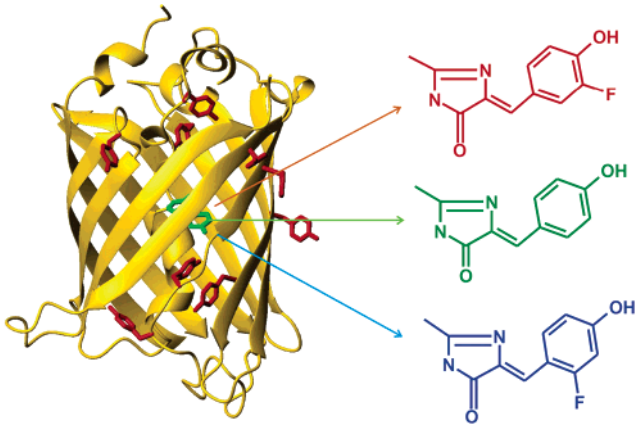

FIGURE 1: General architecture of the *av*GFPs is based on the 11-stranded β-barrel that rigidly holds a chromophore (Cro66) anchored to a coaxial helix within the core of the protein structure. "Enhanced green" *av*GFP (EGFP) contains 11 Tyr residues, with Tyr66 being an integral part of the chromophore. "Enhanced yellow" *av*GFP (EYFP) has an additional Tyr residue at position 203 which is coplanar and about 3.5 Å from the chromophore. Global replacement of Tyr residues in both proteins by (2-F)Tyr and (3-F)Tyr results in a concomitant fluorination of the chromophores.

achieved by subjecting the auxotrophic host cells to an efficient selective pressure without changing their translational components, since the cellular uptake mechanisms as well as aminoacyl-tRNA synthetases as crucial enzymes in the interpretation of the genetic code are incapable of distinguishing between structurally and chemically similar amino acids under the defined conditions (*8*, *9*).

We expected that the fluorine-containing chromophores of *av*GFPs would represent unique probes to study the structure/spectral function relationships in this family of proteins. The chromophore of the *av*GFPs is formed autocatalytically in the post-translational reaction of residues Ser65, Tyr66, and Gly67, with oxygen being the only external requirement (*10*). Since fluorine is the most electronegative element, the C−F bond has dramatically different electronic properties when compared to the C−H bond; i.e., its polarity is opposite that of a C−H bond (*11*). Therefore, the isosteric replacement of hydrogen with fluorine in *av*GFP chromophores as well as in their environment is expected to be accompanied by various changes in their optical properties (*12*).

The "enhanced green fluorescent protein" (EGFP, Phe64Leu/Ser65Thr) (*13*) contains 11 Tyr residues, with Tyr66 being an integral part of the chromophore (Figure 1), and the "enhanced yellow fluorescent protein" (EYFP, Ser65Gly/Val68Leu/Ser72Ala/Thr203Tyr) as the most red-shifted *av*GFP mutant ($\lambda_{em} = 527$ nm) contains an additional Tyr at position 203 (occupied by threonine in wt-*av*GFP) which is located in close proximity (about 3.5 Å) to the chromophore as observed in its X-ray structure (*14*). In the newest modeling studies on EGFP and EYFP a possible explanation of the different populations of the AH and A^- states in these mutants was attempted by comparing the hydrogen-bonding network around their chromophores and showed that the AH/A^- equilibrium involves different internal dynamics with conformational changes of the residues Glu222 and Thr65 (*15*, *16*).

Recently, we serendipitously discovered the coexistence of chromophore isomers (i.e., two rotameric species with nearly equal population distribution) in the crystalline state of 3-fluorotyrosyl-EGFP (*17*). This prompted us to further expand this experiment by global replacement of Tyr side chains in both EGFP and EYFP with (2-F)Tyr and (3-F)Tyr (Figure 1). Subsequent protein crystallization yielded a novel high-resolution X-ray structure of 2-fluorotyrosyl-EGFP, while the effects of fluorination in EYFP variants could only be studied using modeling experiments. These structural data were supplemented by systematic investigations of the pH dependency of the spectral properties using UV absorbance and steady-state fluorescence spectroscopy.

MATERIALS AND METHODS

Chemicals, Bacterial Strains, and Media for Growth. (2-F)Tyr was purchased from Chemos, and other chemicals were puchased from Sigma or Aldrich unless stated otherwise. Replacement experiments were carried out by the use of the Tyr-deficient *E. coli* strain AT2471 (λ^-, *tyrA4*, *relA1*, *spoT1*, *thi*$^{-1}$) from the *E. coli* Genetic Stock Center of Yale University, New Haven, CT. Basic fermentation conditions and medium preparations were performed as described elsewhere (*18*).

Growth, Culture Conditions, Expression, and Purification of Labeled Proteins. The protein expression experiments were performed by using bacterial cultures grown in new minimal medium (NMM) (*19*) in the presence of 100 mg/L ampicillin and 70 mg/L kanamycin. In this medium 0.03 mM L-Tyr was used as the optimal limiting concentration of the native substrate. This provided enough "healthy" cells before depletion of L-Tyr in the mid-logarithmic phase of growth (OD_{600} about 0.5−0.6)—an optimal point at which the noncanonical substrate is added and target protein expression is switched on by addition of IPTG. The culture fermentation after the induction of protein synthesis was 4 h or overnight at 30 °C.

The *E. coli* strain AT2471 was transformed with two plasmids, the ampicillin-resistant pQE60 (Qiagen) harboring Nt-His-tagged EGFP and EYFP gene sequences (BD Biosciences) and kanamycin-resistant pREP4 (Qiagen) containing a repressor gene, *lacI*^{q}. Expressions of both (2-F)Tyr and (3-F)Tyr variants produced soluble proteins in yields similar to those of the parent protein (10−30 mg/L). Parent proteins and (2-F)Tyr- and (3-F)Tyr-containing *av*GFPs were purified by two successive chromatographic steps: (i) Ni−NTA agarose (Qiagen) via an imidazole gradient (0−100 mM) in 100 mM sodium phosphate buffer, pH 8.0, and 0.5 M NaCl and (ii) Phenyl-Sepharose (Pharmacia) with an ammonium sulfate gradient of 20−0% in 20 mM Tris−HCl, pH 8.0, and 1 mM EDTA. The purity of the proteins was assessed by SDS/PAGE, HPLC, and ESI-MS.

UV Absorbance. The UV absorption spectra of protein samples were recorded between 250 and 550 nm on a Perkin-Elmer Lambda 17 UV/vis spectrophotometer. Before the measurements, protein stock concentrations (10−20 mg/mL) were diluted to 0.2−0.4 mg/mL with the appropriate buffer (for different pH values) and allowed to equilibrate for 1 h at room temperature.

Molar extinction coefficients (ϵ_M) measured at 20 °C in neutral buffers for the Tyr + Trp absorption region were determined as described elsewhere (*20*), while chromophore extinction coefficients were derived by normalization to these

Table 1: Absorbance Parameters of EGFP and EYFP and Their Related Variants Produced by Tyr Replacements[a]

protein	Trp + Tyr absorbance		chromophore (Cro66) absorbance		ϵ_M(Cro66)/ ϵ_M(Tyr + Trp)
	ϵ_M (λ_{max})	λ_{max}	ϵ_M (λ_{max})	λ_{max}	
EGFP	19800 (±680)	277	34340 (±1180)	488	1.75
(2-F)Tyr-EGFP	19750 (±917)	271	22190 (±1174)	482	1.13
(3-F)Tyr-EGFP	17930 (±699)	274	30200 (±1200)	485	1.56
EYFP	20900 (±475)	277	48770 (±1250)	514	2.34
(2-F)Tyr-EYFP	20400 (±730)	273	55460 (±2180)	504	2.71
(3-F)Tyr-EYFP	21500 (±590)	274	48790 (±1440)	518	2.26

[a] Absorption maxima (λ_{max}, nm) and molar extinction coefficients (ϵ_M, $M^{-1}cm^{-1}$) are determined in 50 mM sodium phosphate (pH 7.6) in the presence of 100 mM NaCl at room temperature. The experimental conditions are described in the Materials and Methods, and related spectra are presented in Figure 2.

Table 2: Fluorescence Excitation (λ_{exc})[a] and Emission (λ_{em})[a] Values and Their Relative Intensity (RF)[b] Values at 20 °C for the Parent and Variant Proteins[c]

protein	λ_{exc}	λ_{em}	RF	pK_a
EGFP	488	510	1.0	5.74 (±0.15)
(2-F)Tyr-EGFP	482	504	0.6	5.54 (±0.17)
(3-F)Tyr-EGFP	485	514	0.9	5.30 (±0.12)
EYFP	514	527	1.0	6.62 (±0.08)
(2-F)Tyr-EYFP	504	520	1.2	6.52 (±0.10)
(3-F)Tyr-EYFP	518	533	1.0	5.30 (±0.05)

[a] Expressed in nanometers. [b] RF values are normalized to 1.0 and represent the fluorescence intensity of the EGFP and EYFP proteins at standard experimental conditions (25 °C; 50 mM sodium phosphate, pH 7.6, 100 mM NaCl). [c] Under the same conditions pK_a values of their chromophores were determined by fluorescence titration (each value is an average of at least two measurements). The experimental conditions are described in the Materials and Methods, and some of the related spectra are presented in Figure 2.

values (Table 1). The ratio of the chromophore and Tyr + Trp absorbances, $\epsilon_{M(Cro66)}/\epsilon_{M(Tyr+Trp)}$, is usually used as the purity index of *av*GFPs, (*21*) and is about 1.7 for EGFP and 2.3 for EYFP. This ratio differs among parent proteins and their variants due to the effect of fluorine on the formation of the chromophore. Protein variants that are more prone to aggregation such as (2-F)Tyr-EGFP are also characterized by lower values of the $\epsilon_{M(Cro66)}/\epsilon_{M(Tyr+Trp)}$ ratio.

Fluorescence. Fluorescence spectra were recorded in PBS on a Perkin-Elmer spectrometer (LS50B) equipped with digital software. The emission spectra of the protein samples (0.25 μM) were determined upon excitation (495−550 nm, slit 2.5 nm) using the parameters and experimental conditions described in Table 2.

Mass Spectrometry. The extent of Tyr replacement by fluorinated counterparts in the *av*GFP variants was determined by ESI-MS with an ESI PE SCIEX API 165 (Perkin-Elmer) single-quadrupole mass spectrometer. Deconvoluted mass spectra were as follows: parent EGFP (11 Tyr residues), 27743 (±5.0) Da (expected mass 27740.4 Da); (2-F)Tyr-EGFP, 27940 (±4.5) Da; (3-F)Tyr-EGFP, 27938 (±2.5) Da (expected mass in both cases 27941.0 Da); parent EYFP (12 Tyr residues), 27791 (±3.0) Da (expected mass 27790.6 Da); (2-F)Tyr-EYFP, 28008.0 (±6.5); (3-F)Tyr-EYFP, 28005.5 (±3.5) (expected mass in both cases 28006.6 Da).

Fluorescence pH Titration of the Chromophore. Degassed and argon-saturated aqueous solutions were prepared in 100 mM NaCl and 50 mM buffer (citric acid/Na_2HPO_4 (pH 3.0, 3.5), sodium acetate/acetic acid (pH 4.5, 5.0, 5,5), Na_2HPO_4/NaH_2PO_4 (pH 6.0, 6.4, 6.8, 7.2, 7.6, 8.0), boric acid/NaOH (pH 9.0), sodium borate/NaOH (pH 8.5, 9.0, 9.5)). Fluorescence spectra were recorded on a Perkin-Elmer spectrometer (LS50B) equipped with digital software using the "Read-Intensity" option (integration time 3 s). Protein samples (0.25 μM) were examined in the pH range from 1 to 9.5 in different buffers. Probes were excited at different wavelengths (each having a slit width of 2.5 nm), and the intensities of the emission spectra were recorded at the corresponding emission maximum values as described in Table 2.

X-ray Crystallography and Molecular Modeling. The crystallization and structure elucidation procedures of the fluorinated EGFP variants are available in the Supporting Information, while attempts to crystallize either (2-F)Tyr-EYFP or (3-F)Tyr-EYFP were not successful in our hands. Characterization of possible structural effects of the (2-F)-Tyr-EYFP and (3-F)Tyr-EYFP was performed using the crystal structure coordinates of EYFP [PDB ID 1YFP] (*14*). To construct the fluorinated model of EYFP, hydrogen atoms at position 2 (*ortho*) or 3 (*meta*) of the phenyl ring of the chromophore (Cro66) and Tyr203 were replaced with fluorine atoms using options available in the SYBYL package (www.tripos.com). Energy minimization was performed using the Tripos force field with Gasteiger−Hückel charges (*22*). Intramolecular interactions between the chromophore and the protein matrix were analyzed using WebLab Viewer v3.2 (www.accelrys.com) and LIGPLOT v4.4.2 (*23*). However, it should always be kept in mind that the modeled chromophore structures are based on atom coordinates of the parent EYFP, without accounting for possible perturbations induced by fluorination of both the chromophore and neighboring Tyr203.

RESULTS

Absorbance and Fluorescence of Fluorinated EGFPs and EYFPs at Neutral pH. Global replacements of all Tyr side chains in both proteins are reflected in their UV spectra (Table 1, Figure 2). The blue shifts (3−6 nm) of the chromophore absorption are observed in all variants except for (3-F)Tyr-EYFP, whose spectrum is red-shifted by 4 nm when compared to that of the parent protein. Fluorescence emission maxima of the (2-F)Tyr proteins are blue-shifted, while those containing (3-F)Tyr are red-shifted with an enhancement in intensity observed for the EYFP variants at a neutral pH (Table 2). The relative fluorescence and the molar extinction coefficient (ϵ_M) of the (3-F)Tyr-EYFP when compared with parent EYFP were almost unchanged, although they were increased by approximately 15% in the (2-F)Tyr-EYFP protein variant. Moreover, a remarkable reduction (about 35%) in the absorption and the emission

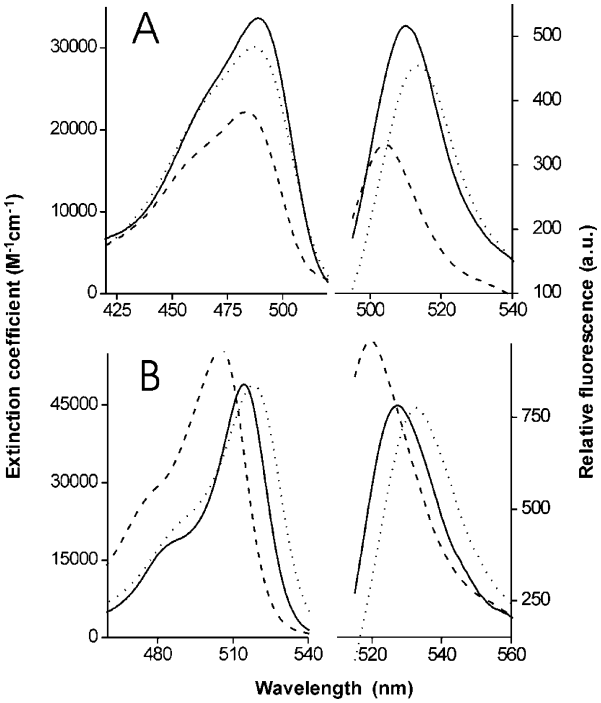

FIGURE 2: (A) Spectral effects upon global fluorination of the Tyr residues in EGFP. The absorption maxima of both fluorinated variants are only slightly blue-shifted when compared to that of the parent protein (full line). In contrast, the fluorescence emission maximum of (2-F)Tyr-EGFP (dashed line) is blue-shifted while that of (3-F)Tyr-EGFP (dotted line) is red-shifted for 6 nm. (B) Global replacement of EYFP with (3-F)Tyr (dotted line) does not change the absorption and emission intensities, while (2-F)Tyr-EYFP (dashed line) exhibits even increased spectral intensities when compared with the parent protein (full line). On the other hand, the maxima for both the absorbance and the fluorescence for (3-F)Tyr-EYFP are red-shifted and those for (2-F)Tyr-EYFP are blue-shifted to a much higher extent than those of EGFP variants (see Tables 1 and 2). The chromophore extinction coefficients of EGFP are derived by normalization to the values at 277 nm (Tyr + Trp spectral region) while fluorescence emission spectra were generated upon excitation at the chromophore region as described in the Materials and Methods.

intensities of (2-F)Tyr-EGFP was observed when compared with those of the parent protein (Tables 1 and 2). The lower ϵ_M values in the order EGFP > (3-F)Tyr-EGFP > (2-F)-Tyr-EGFP correspond well to the reduced intensities in their fluorescence emission spectra (Figure 2). Interestingly, globally fluorinated "enhanced cyan fluorescent protein" (ECFP, Ser65Thr/Tyr66Trp) (*13*, *24*), which contains 10 Tyr residues with the 11th one replaced with Trp at position 66 (chromophore), displays no difference in the spectral properties (shifts, intensities) between the parent protein and fluorotyrosyl variants in either the native or denatured state (see the Supporting Information).

pH Dependence of the Absorption and Fluorescence Properties of the Parent and Fluorinated Proteins. The UV absorption of wt-*av*GFPs is characterized by a complex spectrum comprising two peaks (395 and 475 nm), a feature which has been assigned to the chromophore phenolic oxygen in its protonated (neutral, AH) or deprotonated (anionic, A^-) state (*25*, *26*). While the absorption spectra of the parent EGFP and EYFP are strongly pH dependent, this tendency is less pronounced in their fluorinated variants, with the (2-F)Tyr-EYFP being an exception (Figure 3). The basic features of EGFP, EYFP, and (2-F)Tyr-EYFP include similarities in both the absorption and excitation spectra in the pH range 8.5−10.5. By lowering the pH, the absorptions at 488 nm (EGFP) and 515 nm (EYFP) are decreased, while in nonfluorescent species it is accompanied by an increase in the intensity at 395 nm. The pH dependence of the UV spectra of both parent proteins and their fluorinated variants is characterized by an isosbestic point at 425 nm (Figure 3), indicating a single protonation/deprotonation process as was demonstrated in earlier studies (*27*, *28*). In addition, the fluorinated AH chromophores of denatured protein variants at pH 1.0 show no shift of the absorption profiles (λ_{max} = 378 nm) when compared with parent EGFP and EYFP proteins. In contrast, at higher pH (11.0) a uniform blue shift upon fluorination [λ_{max}(parent proteins) = 447 nm, λ_{max}((2-F)Tyr variants) = 444 nm, λ_{max}((3-F)Tyr variants) = 443 nm] is observed. This would suggest that the spectral shifts represent an intrinsic property of fluorinated A^- chromophores (see the Supporting Information).

The fluorescence emission intensity of *av*GFPs is extremely sensitive to pH alterations, dropping to zero at very low and high pH values, as shown by the pH dependencies of all the protein samples (Figure 4). A fit for one titratable group of the fluorescence emission intensity versus pH shows that fluorination of EGFP in the *ortho* (2-F) position decreases the pK_a value by about 0.2 pH unit, while the fluorine in the *meta* (3-F) position further decreases the pK_a by about 0.5 pH unit. Correspondingly, fluorination of the EGFP chromophore in the *ortho* or *meta* position affects significantly the protonated (AH) species of these variants. But there is no regularity in the absorbance profiles of the (2-F)Tyr-EGFP variant (Figure 3), which is also more prone to aggregation than EGFP and (3-F)Tyr-EGFP.

The EYFP is characterized by a pK_a value of 6.6, which is almost one pH unit higher than that of EGFP (5.7). Fluorination of both the chromophore and Tyr203 in the *meta* (3-F) position is most probably the main cause for the considerable decrease in the pK_a value from 6.6 (parent protein) to 5.3 in (3-F)Tyr-EYFP, as well as for the suppression of its AH species appearance at lower pH values. The (3-F)Tyr-EYFP is more prone to aggregation than EYFP and (2-F)Tyr-EYFP upon longer storage at 4 °C. Conversely, the pH dependence of absorbance and fluorescence and the pK_a value of (2-F)Tyr-EYFP are quite similar to those of the parent EYFP (Table 2).

Fluorinated Tyrosines in the Crystal Structures of (2-F)-Tyr-EGFP and (3-F)Tyr-EGFP. To assess a possible structural basis for the spectral behaviors of fluorinated *av*GFPs, crystallization trials were performed. The (3-F)Tyr-EGFP and (2-F)Tyr-EGFP variants produced crystals that are essentially isomorphous to the Ser65Thr GFP (*29*, *30*) at neutral pH. The crystal structure was determined by molecular replacement and refined at 2.2 Å for (2-F)Tyr-EGFP. We have also collected data for (3-F)Tyr-EGFP at 1.6 Å resolution. Since an inspection of the initial electron densities revealed no differences from that of the already available structure (*17*), the refinement procedure was not performed.

Earlier studies on the spatial structures of (3-F)Tyr-containing proteins show that fluorine atoms are possibly involved in various interactions that can be derived from crystallographic distances. These include possible weak hydrogen bonds with crystallographically well-defined water molecules, other residues, or residues from a symmetry-

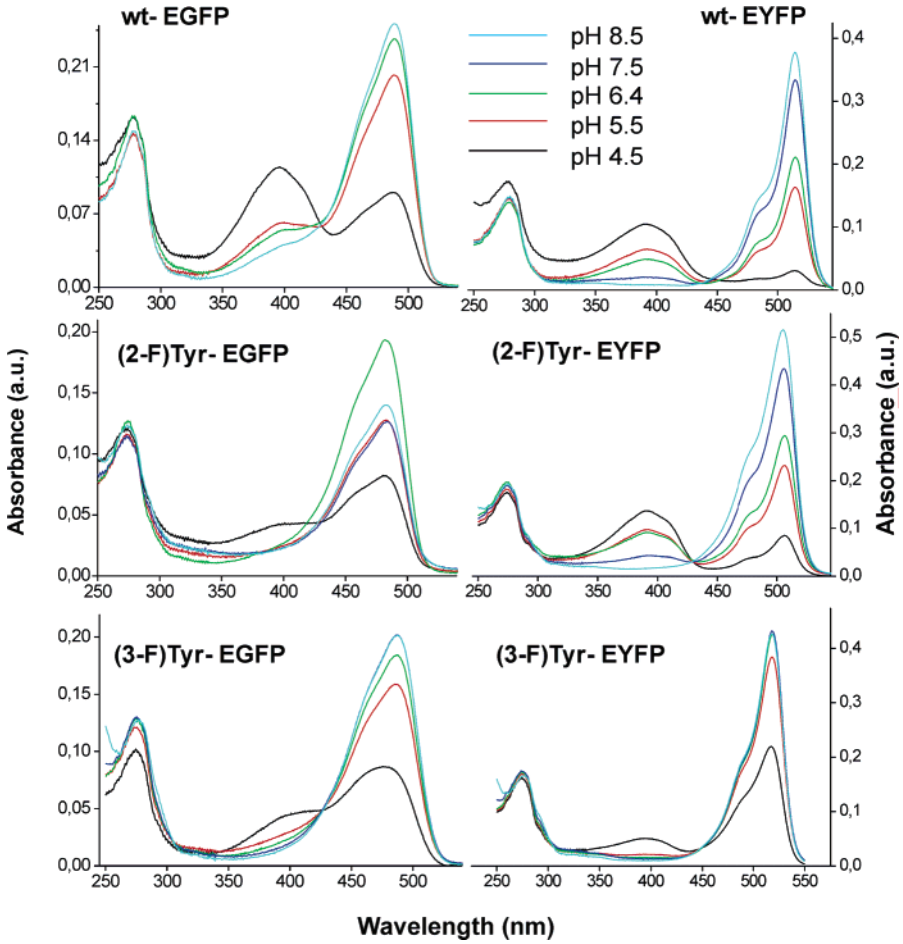

FIGURE 3: pH dependence of the absorption of parent *av*GFPs and their fluorinated variants in 100 mM NaCl and 50 mM buffer solutions. In both parent EYFP and the (2-F)Tyr variant, lowering the pH leads to a decrease in absorbance at 480 and 515 nm (deprotonated form, A^-), and a concomitant increase at 398 nm (protonated form, AH) with a clear isosbestic point in parent proteins. Conversely, the increase in absorption of the protonated form upon a decrease in pH is suppressed in most of the fluorinated protein variants. For experimental conditions and buffer compositions see the Materials and Methods.

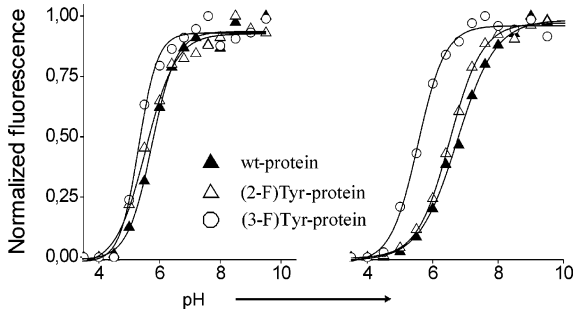

FIGURE 4: Influence of the chromophore fluorination on fluorescence pH titration profiles in parent and variant EGFPs (left) and EYFPs (right). The data points were fitted to a theoretical titration curve with one titratable group since the absorption titration revealed only one isosbestic point (Figure 3). Calculated pK_a values are presented in Table 2; the experimental conditions are described in the Materials and Methods.

related molecule and even numerous unusual interactions (*31*). Our initial structure at a resolution of 2.1 Å (*17*) and the high-resolution structure of (2-F)Tyr-EGFP presented in this study confirm these initial observations. However, it should always be kept in mind that, with its low polarizability and tightly contracted lone pairs, fluorine is unable to compete with stronger hydrogen-bond acceptors such as oxygen and nitrogen (*11*).

Among the 11 Tyr side chains in EGFP, Tyr39, Tyr151, Tyr182, and Tyr200 are surface-exposed, while Tyr143 is only partially exposed to the bulk solvent. Buried in the protein core are Tyr106, Tyr74, Tyr145, and Tyr92. On the other hand, Tyr182 is fully exposed, and no electron density is observed for the fluorine atom due to the high *B* factor (44.20 $Å^2$), while partially exposed Tyr143 assumes both conformeric states, but without detectable distances that might indicate its involvement in particular interactions. The buried residues Tyr74, Tyr106, and Tyr145 are tightly packed in the protein interior, and their fluorine atoms assume only a single conformation (see the Supporting Information). This agrees with the common assumption that the ring-flipping of aromatic residues correlates with their burial in the proteins' molecular cores. In addition, the fluorine of (3-F)-Tyr145 has various contacts to neighboring residues such as the water molecule S14 (2.99 Å), which is also in the hydrogen-bonding distance to the fluorine as well as to the hydroxy group (2.76 Å) of the same residue (Figure 5). The fluorine in the single conformation of (3-F)Tyr106 is 2.95 Å from the ring carbons of Phe130. In contrast, (3-F)Tyr92 although buried exhibits both conformations, one of them in an interaction distance of 2.79 Å with an amide oxygen of Phe84; it is probably in contact also with the ring carbon of Phe84 through a cation$-\pi$ interaction (3.71 Å).

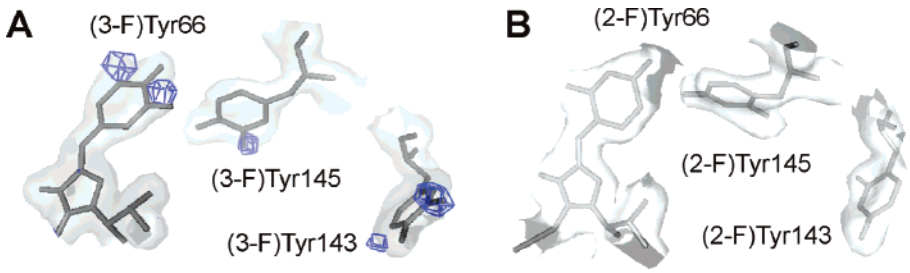

FIGURE 5: X-ray crystallographic structure analysis of the fluorinated chromophores in EGFP variants. The chromophore with a tyrosyl moiety (Tyr66) and residues Tyr145 and Tyr143 are presented as sticks in the same color. The difference Fourier maps (blue, $F_o - F_c$; contouring levels 3.0σ) are superimposed on its continuous electron density ($2F_o - F_c$; contouring level 1 σ). (A) Note the existence of two conformations of the fluorine atom in the (3-F)Tyr-EGFP chromophore. The crystallographic occupancy (i.e., intensities of electron densities) is higher (about 60%) for one conformer (assigned as "major") than for the other (40%, "minor"). While (3-F)Tyr145 has only one conformer, the electron densities of the fluorine atoms of neighboring (2-F)Tyr143 indicate two conformeric states. (B) The fluorine in the chromophore of (2-F)Tyr-EGFP as well as in neighboring fluorotyrosines is characterized by a well-defined electron density at the H → F replacement site in a single conformeric state (well-defined by the $2F_o - F_c$ map with a contouring level of 1σ) (see also the Supporting Information).

Contrary to the generally accepted assumptions, the solvent accessibility of an aromatic residue does not automatically mean that it is prone to flipping. For example, the surface-exposed residue Tyr200 assumes only one isomeric form, and its flipping is most probably prevented by its involvement in lattice contacts in the crystalline state. The pair of closely placed surface-exposed residues Tyr151 (two conformers) and Tyr200 (one conformer) are inclined with an angle of about 65°. The fluorine atom of one conformer of the flipping residue Tyr151 is 3.21 and 3.53 Å from the ring carbon atoms of Tyr200. In the single conformer of (3-F)Tyr200 the fluorine atom is relatively apart from both fluorine atoms of the neighboring (3-F)Tyr151.

Our crystal structure of (2-F)Tyr-EGFP at 2.2 Å shows that all (2-F)Tyr residues are present only in a single conformeric state. For example, the fluorine atom in the *ortho* position in (2-F)Tyr145 (*B* factor 16.98 Å^2) is present in only one well-defined conformational state (Figure 5). Obviously, the replacement of an *ortho* hydrogen by fluorine induces comparatively less steric perturbation than it does in the *meta* position. The observation of the exclusive presence of only one conformation in the crystal structure of (2-F)Tyr-EGFP might be explained from a stereochemical perspective (*ortho* or *meta*) or from structural perturbations or a combination of both (vide infra).

Conformation of the Fluorine in the avGFP's Chromophore. The global substitution of the Tyr side chains in EGFP with both (2-F)Tyr and (3-F)Tyr resulted in the direct incorporation of the fluorine nucleus into the chromophore. Both chromophores and their surrounding residues in terms of the crystallographic *B* factors indicate a rather rigid internal architecture in the crystalline state. In fact, the average *B* factors for atoms in the chromophore of both structures are about 15 Å^2, while the *B* factors of the surrounding residues range from 5 to 25 Å^2. The chromophoric fluorine in (3-F)Tyr-EGFP is present in two conformers with only slight variations in their crystallographic occupancy (Figure 5). The hydroxy groups in both conformers of native and fluorinated chromophore interact directly with Thr203 and His148 through hydrogen bonds, and are in hydrophobic contacts with Thr62, Val150, and Phe165. The *m*-fluorine nucleus creates a set of two crystallographically different microenvironments in which it participates in rather unusual interactions that can be derived from crystallographic distances such as Cγ2 of Thr203 and the "major" conformer of fluorine (distance 3.87 Å; see Figure 6). The diversity of possible fluorine interactions is also illustrated in the "minor" conformer of the (3-F)Tyr chromophore, which is in hydrogen-bond distance (2.82 Å) to the hydroxy group of Ser205 and a conserved solvent water (S16, 2.74 Å).

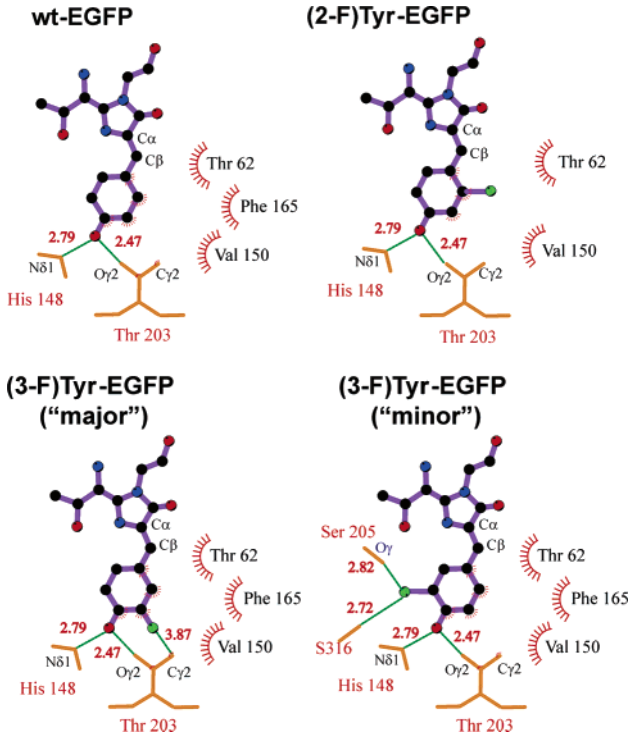

FIGURE 6: Diagrammatic representation of the protein−matrix interactions in parent and fluorinated EGFP variants drawn by LIGPLOT. The hydroxyl group in the chromophore of both native and fluorinated EGFPs directly interacts with Thr203 and His148 through hydrogen bonds, while Thr62, Phe165, and Val150 remain in hydrophobic contact with the chromophore. The single conformer of the (2-F)Tyr chromophore is characterized with a reduced number of hydrophobic contacts. Fluorine, when fitted in the "minor" (3-F)Tyr chromophore conformer, is in hydrogen-bond contact (2.82 Å) with the hydroxyl hydrogen of Ser205 and conserved solvent water (S316, 2.74 Å). On the other hand, Cγ2 of Thr203 is 3.87 Å from the fluorine of the "major" conformer, indicating unusual −CF−HC− interaction.

In contrast, there are no interacting distances of *o*-fluorine in the (2-F)Tyr-containing chromophore with its microenvironment, and even the number of its hydrophobic contacts is reduced (Figure 6). The single conformer that

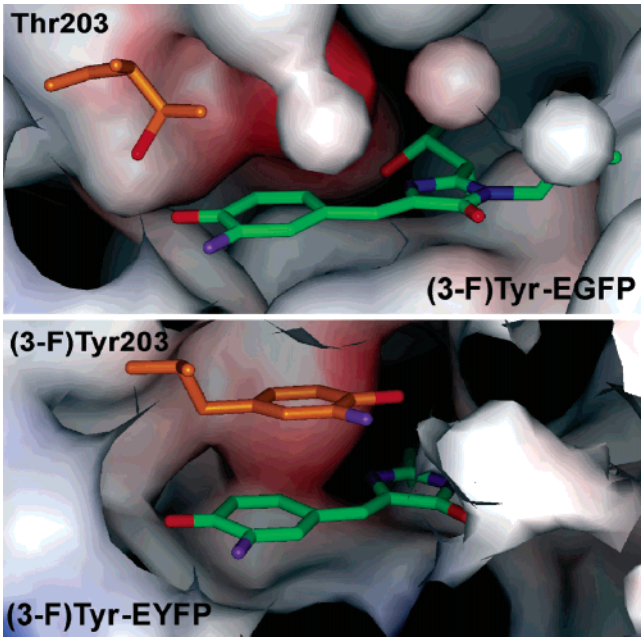

FIGURE 7: Closer inspection of the (3-F)Tyr-EGFP chromophore microenvironment with Thr203 (shown as a stick representation) revealed that there are no sterical hindrances in accommodating the fluorine atom (purple) in the cavity, and even for possible (3-F)Tyr chromophore flipping. The (3-F)Tyr-EYFP model was constructed by the replacement of a hydrogen by a fluorine at Tyr203 and Tyr66 in EYFP, and by a short run of energy minimization (see the Materials and Methods). Although fluorine atoms can easily be accommodated into the EYFP chromophore cavity, it is obvious that chromophore "flipping" should be sterically hindered even in the EYFP structure. The coplanar position of both Tyr203 and (3-F)Tyr203 distant from the center of the chromophore by about 3.5 Å should be the main barrier for possible flipping motions. Molecular surfaces are generated using WebLab Viewer v3.2 (www.accelrys.com). The quantum mechanical modeling and dynamic simulations of chromophore environments of EGFP and EYFP are presented in great detail in refs *15* and *16*.

fluorine exhibits in the chromophore of (2-F)Tyr-EGFP can be plausibly explained by taking into account sterical considerations. Fluorine, when fitted in the "second" *ortho* position of the (2-F)Tyr chromophore, induces a direct clash with the ring nitrogen. In fact, fluorine and nitrogen are approximately 2.1 Å apart. In this way, the exclusive presence of only a single conformer in the fluorinated chromophore of (2-F)Tyr-EGFP could be explained. However, such sterical consideration cannot be applied for all (2-F)Tyr residues throughout the structure (for a more detailed discussion see the Supporting Information). Modeling experiments performed on the atom coordinates of EYFP indicate that fluorine atoms can be inserted into the chromophore and its surrounding protein matrix without causing gross conformational perturbations (Figure 7). However, these modeling data should be considered with precaution since the inability of fluorinated EYFP variants to crystallize under conditions similar to those under which the parent protein crystallizes might be due to the larger structural rearrangements caused by the insertion of fluorine atoms in this microenvironment.

DISCUSSION

The standard amino acid repertoire offers rather limited possibilities for isosteric replacements such as Ser/Ala/Cys, Thr/Val, and Glu/Gln in protein structures. It was recently shown that two isosteric mutations (Thr203Val and Glu222Gln) in wt-*av*GFP selectively increase the energy of both the A^- and AH forms, resulting in the stabilization of an intermediate form (*26*). An expanded amino acid repertoire was expected to further increase these possibilities by providing cellular translation machinery and subsequently target proteins with noncanonical amino acids having "xeno" atoms such as fluorine or chlorine (*9*). In this context, an almost isosteric H → F single-atom exchange in the Tyr residues of protein variants would result in inverted polarities and thus increased charge separation in the chromophore ring. We have recently shown that such structurally isomorphous changes introduced by amino acid analogues and surrogates in *av*GFPs usually have almost no effects on the overall 3-D structure of the protein (*12*), although dramatically changing the spectral and thermodynamic properties in the protein variants (*32*, *33*).

pK_a Changes upon Fluorination. Fluorination of Tyr residues in the *ortho* position lowers the pK_a of the chromophore fluorescence by about 0.2 pH unit in (2-F)-Tyr-EGFP and 0.3 pH unit in (2-F)Tyr-EYFP, while a *m*-fluorine atom in the chromophore of (3-F)Tyr-EGFP is responsible for the decrease of its pK_a by 0.3 pH unit (Table 2). Conversely, the fluorescence pK_a value of (3-F)Tyr-EYFP is decreased by about 1.2 pH units, which could be attributed to the influence of (3-F)Tyr203 in the chromophore vicinity. As the most electronegative element, fluorine is expected to have a significant effect on the acidity or basicity of nearby functional groups, depending upon its position at the aromatic ring. The pK_a lowering of the fluorinated proteins occurs in the order parent protein > (2-F)Tyr variant > (3-F)Tyr variant, which correlates well with the pK_a values of the free amino acids, i.e., Tyr (10.0) > (2-F)Tyr (9.04) > (3-F)Tyr (8.5) (*7*).

Tendency for Aggregation and Appearance of Protonated Species. The chromophore of wt-a*vGFP* is formed autocatalytically from Ser65, Tyr66, and Gly67, and has two major absorption maxima at 395 and 475 nm (*10*). Chromophore formation has been proposed to proceed through a two-step process consisting of a cyclization of the tripeptide Ser65-Tyr66-Gly67 followed by oxidation (*34*−*36*). This intramolecular cyclization requires the proper folding of the surrounding matrix, since the chromophore itself is almost nonfluorescent (*37*, *38*). We observed that the tendency for aggregation of protein variants corresponds well with the suppressability of the appearance of their AH species at lower pH (Figure 3). The incorporation of fluorine was found to produce either favorable or unfavorable effects on correct post-translational chromophore formation and maturation. For example, the tendency for aggregation of (2-F)Tyr-EGFP when compared to that of the parent protein might at least partly be due to the less efficient chromophore maturation or folding of the surrounding matrix. Indeed, both absorbance and fluorescence intensities of this variant are significantly decreased (about 25%, $\epsilon_{M(Cro66)}/\epsilon_{M(Tyr+Trp)} = 1.13$) when compared with those of either EGFP or (3-F)Tyr-EGFP ($\epsilon_{M(Cro66)}/\epsilon_{M(Tyr+Trp)} = 1.75$ and 1.56, respectively). In contrast, (2-F)Tyr as a part of the EYFP chromophore was found to considerably enhance the extinction coefficient and relative fluorescence of this variant ($\epsilon_{M(Cro66)}/\epsilon_{M(Tyr+Trp)} = 2.71$) (Figure 2, Tables 1 and 2), and it is also much less aggregation-prone. Not surprisingly, the (2-F)Tyr-EYFP

samples are relatively resistant toward aggregation over longer periods of time at room temperature as well as at 4 °C.

Intrinsic Spectral Shifts of the Fluorinated Chromophores in EGFP. The complex photophysics of the chromophore, including properties such as optical absorption, fluorescence, and ultrafast dynamic fluorescence properties of the native *av*GFP are explained by the three-state photoisomerization model. It assumes that the chromophore exists in the neutral (395 nm, AH) or in an anionic (475 nm, A^-) state; the latter exists in a thermodynamically unstable intermediate form (493 nm, I state) (*25*, *26*). Structural analysis and quantum mechanical calculations suggest that they represent chromophores with protonated and deprotonated tyrosyl hydroxy groups, respectively (*28*, *39*−*43*).

Fluorine being the most electronegative element is expected to exert strong inductive electron-withdrawing effects on the fluorinated chromophore ring. By this effect the ring becomes relatively electron deficient and more hydrophilic, which makes its hydroxy moiety more acidic. Both excited and ground states of the phenol oxygen of Tyr66 would certainly be influenced by such almost isosteric H → F single-atom exchange. The electron-withdrawing fluorine atom in the *meta* position, since placed in vicinity of the phenol hydroxy group, should enhance the acidity of the (3-F)Tyr chromophore to a larger extent than in the (2-F)Tyr chromophore. In fact, the pK_a of (3-F)Tyr (8.5) is 1.5 pH units lower than the pK_a of Tyr (10.0) (*7*). Correspondingly, the deprotonated anionic A^- state of the chromophore is much more favored upon its fluorination at the *meta* position. This would explain the suppression of the AH species appearance in (3-F)Tyr-EGFP and (3-F)Tyr-EYFP upon lowering the pH (Figure 3), as well as the differences in the pH titration curves (Figure 4).

Introduction of fluorine in the chromophore can give rise to several effects in addition to a decrease in the pK_a value. Red-shifted fluorescence spectra of (3-F)Tyr-containing proteins can be attributed to their stronger induction of the anionic A^- state of the chromophore. (2-F)Tyr-containing proteins are expected to behave likewise. Conversely, fluorescence emission maxima of both (2-F)Tyr-EYFP and (2-F)Tyr-EGFP are blue-shifted (Table 2). It is therefore obvious that there are other factors responsible for these spectral shifts. Besides the electron-withdrawing properties, the resonance and electron-donating effects caused by fluorine as well as by the hydroxy group might influence the electronic properties of the aromatic chromophore ring. These combined effects have to be responsible for red-shifted fluorescence of (3-F)Tyr relative to Tyr, and altered balances of these effects in (2-F)Tyr chromophores have to account for their intrinsic blue shifts in fluorescence. Furthermore, it is likely that the inductive electron-withdrawing effects in the (2-F)Tyr chromophore outweigh the resonance effects to lower extents than in the (3-F)Tyr chromophore. As a result, the biophysical properties of (2-F)Tyr and related chromophores are much more similar to those of the parent structures. In general, H → F atom exchange in tyrosyl moieties not only results in inverted polarities but also affects electron delocalizations as well as orientations of transition- and ground-state dipoles in the chromophore ring (*44*).

Enhanced Blue- and Red-Shifted Fluorescence in Fluorinated EYFP Variants. The hydroxy group of Tyr66 present in the chromophore of wt-*av*GFP is in equilibrium between the protonated (AH) and deprotonated (A^-) states. Contrary to wt-*av*GFP, the "enhanced" mutants (i.e., EGFP and EYFP) possess the Ser65Thr mutation that results in a destabilization of the neutral chromophore (AH**)** and a consequent increase of the anionic chromophoric state (A^-) (*29*). On the other hand, the main difference between EGFP and EYFP is the absence of the Thr203 hydroxy donor, which is replaced by Tyr in EYFP. The removal of Thr203 as an H-bond donor to the phenolate of chromophore causes its less coordination, while insertion of Tyr203 introduces aromatic stacking interaction with the chromophore. It was argued that the aromatic mutant Tyr203 with its ring might stabilize the charge and thus lower the energy of the excited state, leading to an additional red shift when compared to Val203 mutants (*43*). However, molecular dynamic analyses and quantum mechanical calculations based on atomic coordinates of both EGFP and EYFP revealed that the chromophore excitation energy is affected by its hydrogen-bond contacts with the surrounding chromophore matrix independent from a stabilization of its states. These theoretical calculations predict that a hydrogen bond of the carbonyl group of the imidazolinone ring with Arg96 would yield a red-shifting of the A^- chromophore while hydrogen bonding of the chromophore phenol hydroxy group with The203 would cause a blue shift. In this context, the red shift of the EYFP A^- chromophore can be attributed to the (i) removal of Thr203 and (ii) interaction of the chromophore with Tyr203 (*16*).

The enhanced blue and red shifts as well as different spectral intensities in fluorinated EYFPs can be attributed to the fluorination of Tyr203 whose juxtaposition directly affects the mode of its interaction with the fluorinated chromophore. As expected, the fluorescence emission spectrum of (2-F)Tyr-EYFP is blue-shifted by 7 nm ($\lambda_{max} = 320$ nm) when compared with that of EYFP (Table 2). These trends are also observable in the chromophore absorption profile of the fluorinated EYFPs (Table 1, Figure 2). Fluorine atoms in the aromatic ring at position 203 which stacks next to the chromophore are expected to induce an additional polarization in its microenvironment. This might additionally affect $\pi-\pi$ interactions, the ground-state equilibrium of AH and A^- species, charge stabilization, and subsequently the energy levels of the chromophore ground and excited states. The differences observed in related protein mutants might also be attributed to the different stereochemistry of *o*- and *m*-fluorine atoms in Tyr203 relative to the protonated/deprotonated hydroxy moiety of the fluorinated chromophore. Indeed, fluorine is known to exert a strong inductive effect that is sufficient to affect properties such as polarity or binding capacity of functional groups that are even distantly positioned in the structure (*45*). For example, Holmgren et al. attributed the hyperstability of the fluorinated collagen triple helix to the inductive effects introduced by fluorine atoms in its structure (*46*).

Conformation of the Fluorine in the avGFP's Chromophore. The coexistence of two rotameric species in the crystal state with similar populations (Figure 5) raised an interesting question as to whether a flipping of the 3-fluorotyrosyl moiety is plausible. The first diffraction data collected at room temperature in our initial studies (*17*) showed no changes in rotamer population. This observation, together with the absence of direct dynamic evidence of

"flipping", indicates that the distribution of the experimental electron densities of fluorine in the (3-F)Tyr chromophore is rather a result of Tyr-flipping that was "caught" or "frozen" upon chromophore formation and maturation. On the other hand, it was demonstrated that the chromophore may even have the room to adopt some nonplanar geometries in the large central cavity of *av*GFPs; i.e., some rotational freedom to the planar chromophore is allowed (*39*). This is also the case for EGFP, while in the cavity of EYFP the Tyr203 occupies an additional space and its 3-fluorotyrosyl chromophore has no rotational freedom for flipping in the manner observed for the (3-F)Tyr-EGFP chromophore (Figure 7).

ACKNOWLEDGMENT

We thank Gregor Jung and Andreas Zumbusch for a critical reading of the manuscript, Mrs. E. Weyher for mass spectrometric measurements, and Ms. T. Krywcun, Ms. P. Birle, and Mrs. W. Wenger for help in the preparative work. Unknown reviewers are greatly acknowledged for their constructive criticisms and numerous suggestions that considerably improved the quality of this paper.

SUPPORTING INFORMATION AVAILABLE

Fluorescence profiles of native ECFP, EYFP, and EGFP and their fluorinated variants at pH 7 and 10, absorption maxima of chromophores in denatured proteins at low and high pH values, crystallizations, X-ray data collections, and structure elucidation of (2-F)Tyr-EGFP, and microenvironment description of (2-F)Tyr and (3-F)Tyr residues in the related crystal structures. This material is available free of charge via the Internet at http://pubs.acs.org.

REFERENCES

1. Fink, N. (1948) Iodotyrosine and tyroglobulin, *Experimentia 43*, 23−45.
2. O'Hagan, D., Schaffrath, C., Cobb, S. L., Hamilton, J. T. G., and Murphy, C. D. (2002) Biosynthesis of an organofluorine molecule: A fluorinase enzyme has been discovered that catalyses carbon-fluorine bond formation, *Nature 416*, 279−279.
3. Lu, P., Jarema, M., and Mosser, K. (1976) Lac Repressor: 3-Fluorotyrosine Substitution for NMR Studies, *Fed. Proc. 35*, 1456−1456.
4. Sykes, B. D., Weingart, H., and Schlesin, M. J. (1974) Fluorotyrosine Alkaline-Phosphatase from *Escherichia coli*: Preparation, Properties, and Fluorine-19 Nuclear Magnetic-Resonance Spectrum, *Proc. Natl. Acad. Sci. U.S.A. 71*, 469−473.
5. Weissman, A., and Koe, B. K. (1966) Studies on Mechanism of Convulsant Action of DL-*m*-Fluorotyrosine, *Pharmacologist 8*, 215.
6. Budisa, N. (2004) Prolegomena to future experimental efforts on genetic code engineering by expanding its amino acid repertoire, *Angew. Chem., Int. Ed. 43*, 3387−3428.
7. Brooks, B., Phillips, R. S., and Benisek, W. F. (1998) High-efficiency incorporation in vivo of tyrosine analogues with altered hydroxyl acidity in place of the catalytic tyrosine-14 of δ(5)-3-ketosteroid isomerase of *Comamonas* (*Pseudomonas*) *testosteroni*: Effects of the modifications on isomerase kinetics, *Biochemistry 37*, 9738−9742.
8. Budisa, N., Moroder, L., and Huber, R. (1999) Structure and evolution of the genetic code viewed from the perspective of the experimentally expanded amino acid repertoire in vivo, *Cell. Mol. Life Sci. 55*, 1626−1635.
9. Budisa, N., Minks, C., Alefelder, S., Wenger, W., Dong, F. M., Moroder, L., and Huber, R. (1999) Toward the experimental codon reassignment in vivo: Protein building with an expanded amino acid repertoire, *FASEB J. 13*, 41−51.
10. Shimomura, O. (1979) Structure of the Chromophore of Aequorea Green Fluorescent Protein, *FEBS Lett. 104*, 220−222.
11. Dunitz, J. D. (2004) Organic Fluorine: Old man out, *ChemBioChem 5*, 614−621.
12. Budisa, N., Pal, P., Alefelder, S., Birle, P., Krywcun, T., Rubini, M., Wenger, W., Bae, J. H., and Steiner, T. (2004) Probing the Role of Tryptophans in *Aequorea victoria* Green Fluorescent Proteins with an Expanded Genetic Code, *Biol. Chem. 385*, 191−202.
13. Tsien, R. Y. (1998) The green fluorescent protein, *Annu. Rev. Biochem. 67*, 509−544.
14. Wachter, R. M., Elsliger, M. A., Kallio, K., Hanson, G. T., and Remington, S. J. (1998) Structural basis of spectral shifts in the yellow-emission variants of green fluorescent protein, *Structure 6*, 1267−1277.
15. Nifozi, R., and Tozzini, V. (2003) Molecular dynamics simulations of Enhanced Green Fluorescent Proteins: Effects on F64L, S65T and T203Y mutations on the ground state equilibrium, *Proteins 51*, 378−389.
16. Laino, T., Nifozi, R., and Tozzini, V. (2004) Relationship between structure and optical properties in green fluorescent proteins: A quantum mechanical study of the chromophore environment, *Chem. Phys. 298*, 17−28.
17. Bae, J. H., Pal, P. P., Moroder, L., Huber, R., and Budisa, N. (2004) Crystallographic Evidence for Isomeric Chromophores in 3-Fluorotyrosyl-Green Fluorescent Protein, *ChemBioChem 5*, 720−722.
18. Budisa, N., Karnbrock, W., Steinbacher, S., Humm, A., Prade, L., Neuefeind, T., Moroder, L., and Huber, R. (1997) Bioincorporation of telluromethionine into proteins: A promising new approach for X-ray structure analysis of proteins, *J. Mol. Biol. 270*, 616−623.
19. Budisa, N., Steipe, B., Demange, P., Eckerskorn, C., Kellermann, J., and Huber, R. (1995) High-Level Biosynthetic Substitution of Methionine in Proteins by Its Analogs 2-Aminohexanoic Acid, Selenomethionine, Telluromethionine and Ethionine in *Escherichia coli*, *Eur. J. Biochem. 230*, 788−796.
20. Budisa, N., Rubini, M., Bae, J. H., Weyher, E., Wenger, W., Golbik, R., Huber, R., and Moroder, L. (2002) Global replacement of tryptophan with aminotryptophans generates non-invasive protein-based optical pH sensors, *Angew. Chem., Int. Ed. 41*, 4066−4069.
21. Fukuda, H., Arai, M., and Kuwajima, K. (2000) Folding of green fluorescent protein and the cycle3 mutant, *Biochemistry 39*, 12025−12032.
22. Gasteiger, J., and Marsili, M. (1980) Iterative partial equalization of orbital electronegativity: A rapid access to atomic charges, *Tetrahedron 36*, 3219−3228.
23. Wallace, A. C., and Laskowski, R. A. (1995) LIGPLOT: A program to generate schematic diagrams of protein-ligand interactions, *Protein Eng. 8*, 127−134.
24. Palm, G. J., and Wlodawer, A. (1999) Spectral variants of green fluorescent protein, in *Green Fluorescent Protein*, pp 378−394.
25. Brejc, K., Sixma, T. K., Kitts, P. A., Kain, S. R., Tsien, R. Y., Ormo, M., and Remington, S. J. (1997) Structural basis for dual excitation and photoisomerization of the *Aequorea victoria* green fluorescent protein, *Proc. Natl. Acad. Sci. U.S.A. 94*, 2306−2311.
26. Wiehler, J., Jung, G., Seebacher, C., Zumbusch, A., and Steipe, B. (2003) Mutagenic Stabilization of the Photocycle Intermediate of Green Fluorescent Protein (GFP), *ChemBioChem 4*, 1164−1171.
27. Heim, R., Prasher, D. C., and Tsien, R. Y. (1994) Wavelength Mutations and Posttranslational Autoxidation of Green Fluorescent Protein, *Proc. Natl. Acad. Sci. U.S.A. 91*, 12501−12504.
28. Haupts, U., Maiti, S., Schwille, P., and Webb, W. W. (1998) *Proc. Natl. Acad. Sci. U.S.A. 95*, 13573−13578.
29. Ormo, M., Cubitt, A. B., Kallio, K., Gross, L. A., Tsien, R. Y., and Remington, S. J. (1996) Crystal structure of the *Aequorea victoria* green fluorescent protein, *Science 273*, 1392−1395.
30. Yang, F., Moss, L. G., and Phillips, G. N. (1996) The molecular structure of green fluorescent protein, *Nat. Biotechnol. 14*, 1246−1251.
31. Xiao, G. Y., Parsons, J. F., Tesh, K., Armstrong, R. N., and Gilliland, G. L. (1998) Conformational changes in the crystal structure of rat glutathione transferase M1-1 with global substitution of 3-fluorotyrosine for tyrosine, *J. Mol. Biol. 281*, 323−339.
32. Minks, C., Huber, R., Moroder, L., and Budisa, N. (1999) Atomic mutations at the single tryptophan residue of human recombinant annexin V: Effects on structure, stability, and activity, *Biochemistry 38*, 10649−10659.

33. Bae, J. H., Rubini, M., Jung, G., Wiegand, G., Seifert, M. H. J., Azim, M. K., Kim, J. S., Zumbusch, A., Holak, T. A., Moroder, L., Huber, R., and Budisa, N. (2003) Expansion of the genetic code enables design of a novel "gold" class of green fluorescent proteins, *J. Mol. Biol. 328*, 1071−1081.
34. Cubitt, A. B., Heim, R., Adams, S. R., Boyd, A. E., Gross, L. A., and Tsien, R. Y. (1995) Understanding, Improving and Using Green Fluorescent Proteins, *Trends Biochem. Sci. 20*, 448−455.
35. Cody, C. W., Prasher, D. C., Westler, W. M., Prendergast, F. G., and Ward, W. W. (1993) Chemical-Structure of the Hexapeptide Chromophore of the *Aequorea* Green-Fluorescent Protein, *Biochemistry 32*, 1212−1218.
36. Niwa, H., Inouye, S., Hirano, T., Matsuno, T., Kojima, S., Kubota, M., Ohashi, M., and Tsuji, F. I. (1996) Chemical nature of the light emitter of the *Aequorea* green fluorescent protein, *Proc. Natl. Acad. Sci. U.S.A. 93*, 13617−13622.
37. Barondeau, D. P., Putnam, C. D., Kassmann, C. J., Tainer, J. A., and Getzoff, E. D. (2003) Mechanism and energetics of green fluorescent protein chromophore synthesis revealed by trapped intermediate structures, *Proc. Natl. Acad. Sci. U.S.A. 100*, 12111−12116.
38. Bublitz, G., King, B. A., and Boxer, S. G. (1998) Electronic structure of the chromophore in green fluorescent protein (GFP), *J. Am. Chem. Soc. 120*, 9370−9371.
39. Voityuk, A. A., Kummer, A. D., Michel-Beyerle, M. E., and Rosch, N. (2001) Absorption spectra of the GFP chromophore in solution: Comparison of theoretical and experimental results, *Chem. Phys. 269*, 83−91.
40. Helms, V., Straatsma, T. P., and McCammon, J. A. (1999) Internal dynamics of green fluorescent protein, *J. Phys. Chem. B 103*, 3263−3269.
41. Chattoraj, M., King, B. A., Bublitz, G. U., and Boxer, S. G. (1996) Ultra-fast excited state dynamics in green fluorescent protein: Multiple states and proton transfer, *Proc. Natl. Acad. Sci. U.S.A. 93*, 8362−8367.
42. Kummer, A. D., Kompa, C., Lossau, H., Pollinger-Dammer, F., Michel-Beyerle, M. E., Silva, C. M., Bylina, E. J., Coleman, W. J., Yang, M. M., and Youvan, D. C. (1998) Dramatic reduction in fluorescence quantum yield in mutants of Green Fluorescent Protein due to fast internal conversion, *Chem. Phys. 237*, 183−193.
43. Kummer, A. D., Wiehler, J., Rehaber, H., Kompa, C., Steipe, B., and Michel-Beyerle, M. E. (2000) Effects of threonine 203 replacements on excited-state dynamics and fluorescence properties of the green fluorescent protein (GFP), *J. Phys. Chem. B 104*, 4791−4798.
44. Seifert, M. H., Ksiazek, D., Azim, M. K., Smialowski, P., Budisa, N., and Holak, T. A. (2002) Slow exchange in the chromophore of a green fluorescent protein variant, *J. Am. Chem. Soc. 124*, 7932−7942.
45. Marsh, E. N. G., and Neil, E. (2000) Towards the nonstick egg: Designing fluorous proteins, *Chem. Biol. 7*, R153−R157.
46. Holmgren, S. K., Bretscher, L. E., Taylor, K. M., and Raines, R. T. (1999) A hyperstable collagen mimic, *Chem. Biol. 6*, 63−70.

BI0484825